*Smart Structures and Systems, Vol. 2, No. 2 (2006) 155-169*
DOI: http://dx.doi.org/10.12989/sss.2006.2.2.155


# Application of magnetoelastic stress sensors in large steel cables

Guodun Wang†, Ming L. Wang‡, and Yang Zhao‡†

*Department of Civil and Materials Engineering, the University of Illinois at Chicago, Chicago, IL60607, USA*

Yong Chen‡‡ and Bingnan Sun‡‡†

*Department of Civil Engineering, Zhejiang University, Hangzhou, China*

*(Received March 28, 2005, Accepted January 12, 2006)*

**Abstract.** In this paper, the application of magnetoelasticity in static tension monitoring for large steel cables is discussed. Magnetoelastic (EM) stress sensors make contact-free tension monitoring possible for hanger cables and post-tensioned cables on suspension and cable-stayed bridges. By quantifying the correlation of magnetic relative permeability with tension and temperature, the EM sensors inspect the load levels in the steel cables. Cable tension monitoring on Qiangjiang (QJ) 4th Bridge demonstrates the reliability of the EM sensors.

**Keywords:** magnetoelasticity; relative permeability; tension; temperature.

## 1. Introduction

Recognized as necessary by design engineers and licensing authorities, knowledge of tension in steel cables and tendons for pre-stressed concrete structures and cable-stayed bridges is extremely valuable during construction and subsequent structural monitoring. Ideally, these measurements need to be performed rapidly, at low cost, with portable equipment at any time with little or no field preparation. Some researches currently conducted are trying to apply fiber optic sensors and vibration string sensors. However, the problem of durability is still a bottleneck. With theoretically unlimited service life, EM sensor can monitor the tension in steel cable with high-density polyethylene (HDPE) cover, and make contact-free measurement feasible with high accuracy at a comparatively low cost. Therefore, they are drawing an ever increasing attention in load monitoring for steel cables and tendons used in infrastructures.

The magnetic and magnetoelastic properties of ferromagnetic materials can be described according to magnetic domain theory (Weiss 1907). In a demagnetized and unloaded ferromagnetic sample, the domains are arranged randomly, and as a result, there is a net magnetization of zero. When a ferromagnetic

†PhD Candidate, E-mail: gwang5@uic.edu
‡Professor, E-mail: mlwang@uic.edu
‡†Research Scientist, E-mail: zhaoy@uic.edu
‡‡Associate Professor, E-mail: cecheny@zju.edu.cn
‡‡†Professor, E-mail: sbn@zju.edu.cn

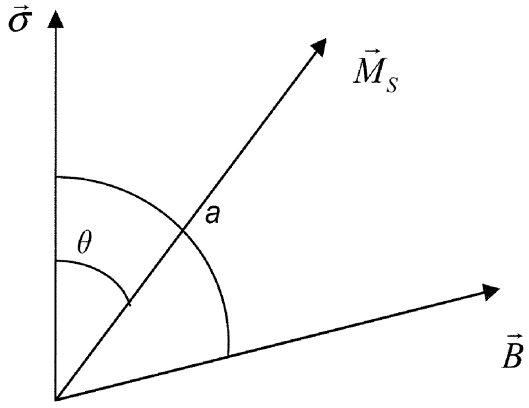


Fig. 1 Magnetic moment under stress

material is subjected to an applied field, the domains rotate and align themselves along the direction of the magnetic field. As a side effect of magnetic hysteresis, Barkhausen noise can be introduced when the material is being magnetized (Bertotti 1992).

It has long been known and extensively studied that stress changes the magnetic properties (Joule 1842, Bozorth 1951, Cullity 1972, Mix 1987, Stablik and Jiles 1993), which is called magnetoelasticity. This phenomenon is caused by the interaction of stress with magnetic domains and magnetic moments, which are discussed below.

### 1.1. Influence of stress on magnetic moment rotation

Stress can rotate the magnetic moments due to magnetoelastic energy. For a small sample with uniaxial magnetic moment $M_S$, stress $\sigma$ is applied along the direction with angle $\theta$ from the magnetic moment. The easy direction for all the other anisotropies combined is along $B$, with angle $\boldsymbol{a}$ from stress, as indicated in Fig. 1.

The stress anisotropic energy is

$$E_{me} = \frac{3}{2}\lambda_s \sigma \sin^2\theta \tag{1}$$

where $\lambda_s$ is saturation magnetostriction constant. The combined energy from all the other anisotropies is

$$E_{other} = K\sin^2(\alpha - \theta) \tag{2}$$

where $K$ indicates the overall anisotropy constant.

With stress applied, the magnetic moment will rotate until the thermodynamic equilibrium is achieved. Under thermodynamic equilibrium, the following requirements must be fulfilled:

$$d\left(\frac{3}{2}\lambda_s \sigma \sin^2\theta + K\sin^2(\alpha - \theta)\right)/d\theta = 0 \tag{3}$$

and

$$d^2\left(\frac{3}{2}\lambda_s \sigma \sin^2\theta + K\sin^2(\alpha - \theta)\right)/d\theta^2 > 0 \tag{4}$$

### *1.2. Influence of stress on domain wall movement*

Stress behaves as a fictitious force working on the domain walls (Birss 1971). We can consider there is a small specimen comprised of four domains with negative magnetostriction, as indicated in Fig. 2. Arrows within domains indicate the direction of saturated magnetization - $M_s$. The volumes of the domains with magnetic moments that are not parallel to the tension increase at the expense of the volume of domains with moments parallel to the tension, in order to reduce the magnetoelastic energy. To describe the stress-induced wall movement, 90° walls and 180° walls are to be considered separately. For the 90° walls, the moving distance is controlled by the balance of the pressure exerted by magnetic field and stress (Cullity 1972), as given in the following equation:

$$dE/dx = -HM_S + \frac{3}{2}\lambda_S g x \tag{5}$$

where $E$ is the total energy per unit volume within the domain, $g$ refers to the stress gradient along the wall sliding direction, and $x$ indicates the sliding distance. However, for 180° walls, the magnetoelastic energy is zero according to Eq. (1), as $\theta = 0°$. Therefore, the equilibrium of magnetic potential energy and domain wall energy determines the sliding distance of the 180° wall.

From the aforementioned theories, it is observed that tensile stress reduces the magnetization level of the material with negative magnetostriction, provided the external field is parallel to the stress, as shown in

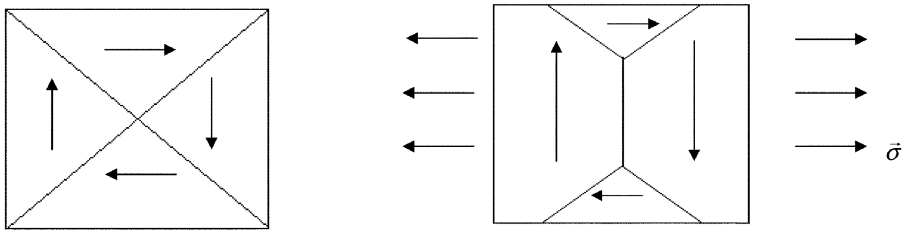


Fig. 2 Domain wall movement under stress in the material with negative magnetostriction, left – under zero stress, right – under uniaxial stress $\sigma$

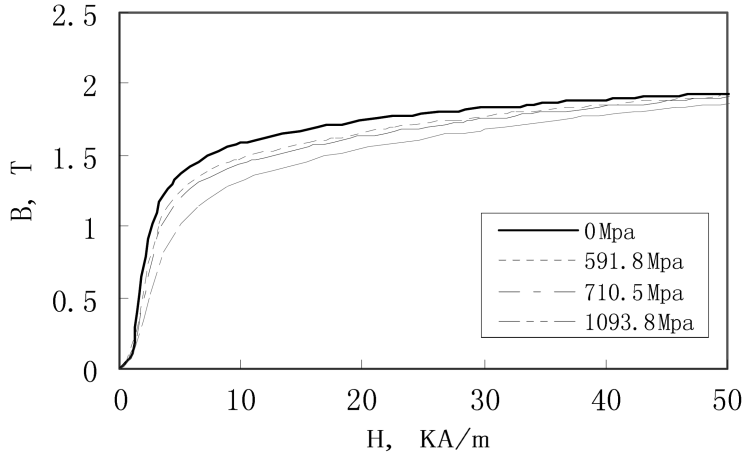


Fig. 3 Initiative hysteresis curves of the 7 mm piano steel wires under various uniaxial stress levels

Fig. 3. The applied stress also changes the energy of the imperfections and impurities which pin the domain walls.

The magnetoelasticity can be described in the following expression (Bozorth 1951):

$$\frac{1}{l}\frac{\partial l}{\partial H} = \frac{1}{4\pi}\frac{\partial B}{\partial \sigma} \tag{6}$$

where $l$ is length of the sample, $B$ is induction. Eq. (6) indicates that tension leads to the increase of induction, provided the material considered is of positive magnetostriction.

From Eq. (6) there is (Jiles and Ho 2003):

$$\left(\frac{dB}{d\sigma}\right)_H = \left(\frac{d\lambda}{dH}\right)_\sigma = \frac{d\lambda}{dM}\frac{dM}{dH} = \frac{2\mu_0 M_S}{N}\left(\frac{\lambda_S}{K}\right) \tag{7}$$

where $K$ means magnetic anisotropy constant and $N$ is a material constant (for steel it is 3). $\lambda_S$ remains the same as in Eq. (1).

Researchers and engineers have explored the application of magnetoelasticity in non-destructive evaluation of the infrastructures (Mix 1987, Wang and Koontz, *et al.* 1998, Daughton 1999, Tayalia and Heider, *et al.* 2000, Wang and Lloyd, *et al.* 2001, Singh and Lloyd, *et al.* 2003). With the steel rod to be monitored as the sensing part, the EM stress sensor is aimed at characterizing the stress dependence of the apparent relative permeability which can be derived from (Wang and Chen 2000):

$$\mu_{ar}(\sigma, T, H) = 1 + \frac{A_0}{A_f}\left(\frac{V_{out}(\sigma, T, H)}{V_0} - 1\right) \tag{8}$$

where $V_{out}$ indicates the integrated secondary voltage with rod in the solenoid, and $V_0$ is the integrated voltage without rod in the solenoid. The permeability is measured under technical magnetic saturation, in order to diminish the effect of eddy current and achieve a uniform magnetization within the material. In this research, the temperature and stress dependence of the apparent relative permeability is revealed through calibration. During *in situ* tension monitoring, the tension can be calculated by measuring the temperature and relative permeability. Besides permeability, the magnetic flux variation introduced by stress within the material can also be used in tension monitoring (Wang and Wang 2004).

EM sensors are currently applied to cylindrical cables with constant diameters. For the cable with irregular cross section or heavily corroded, the EM sensor can reflect the stress variation, given the cross section of the cable at the sensor location is known. Researches are currently conducted at the University of Illinois at Chicago (UIC) in order to directly measure corrosion and fatigue of the steel cable using the variation in magnetic induction and magnetic field.

## 2. Qiangjiang 4th bridge

QJ 4th Bridge, on Qiangjiang river in Hangzhou of China, 27.6 meters wide and 1376 meters long, is China's longest double-deck, multi-arch bridge with multiple utilities. It is composed of two 190-meter-long big arches and nine 85-meter-long small arches. The upper deck is a six-lane highway and on the lower deck there are a railway and sidewalks for pedestrians and bicycles. The bridge under construction is shown in Fig. 4. To evaluate the service reliability of the bridge, a state-of-the-

Fig. 4 Picture of QJ 4th Bridge under construction

art health monitoring system was employed, including the EM stress sensors, which were mounted on critical hanger cables and post-tensioned cables on two big arches and one small arch. The main reasons for the selection of EM sensors are easy mounting, no contact to the cable even with HDPE sheath, and for long term durability. Load cells were mounted temporarily at the anchor positions during construction for loading control and short-term verification.

## 3. Equipment and measurement setup

EM sensor is operated with the PowerStress Measurement System (PSM System). The PSM system is composed of energizing current supply, signal-filtering hardware and data-analysis software, which was

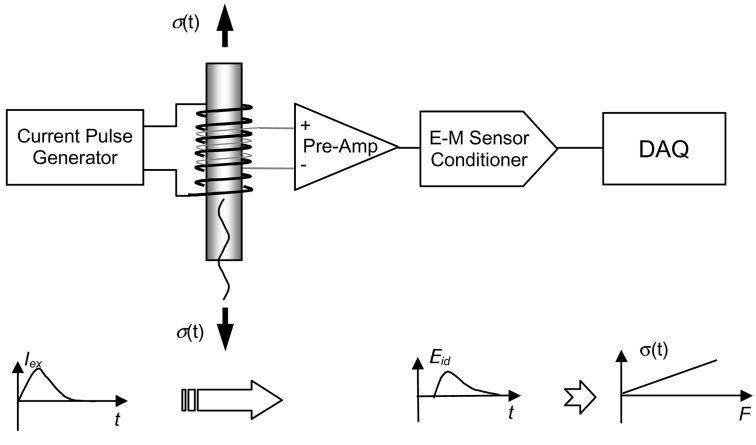


Fig. 5 Indicative working chart of PowerStress Measurement System developed in the Infrastructures Sensor Technology Laboratory of UIC

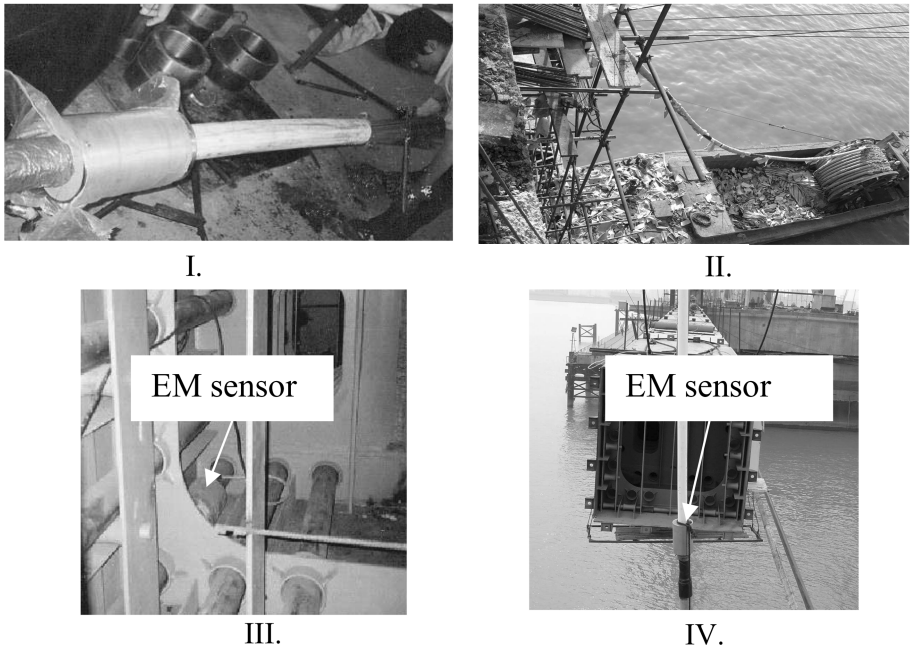


Fig. 6 Pictures of EM sensors and cables, I-Sensor mounted on hanger cable, II. Post-tensioned cable being installed into the box girder, III. post-tensioned cable with EM sensor in box girder, IV-Hanger cable with EM sensor

innovated at the Infrastructures Sensor Technology Laboratory of UIC. The PSM System can principally undertake the following tasks:

(1) It generates a large pulsed current to magnetize the steel cable.

(2) It picks up the analog signals from the primary coil, secondary coil, and temperature sensor.

(3) Each unit sequentially manipulates dozens of EM stress sensors through multiplexers and logic switches.

The working chart of the PSM System is shown in Fig. 5.

EM sensors can be used in stress monitoring for small strands and big cables. In QJ 4th Bridge, there are four types of big cables that need to be monitored: 109×7 mm hangers, 85×7 mm hangers, 55×7 mm hanger cables and 37×15.5 mm post-tensioned cables. All the cables were made of high-strength steels, but the tensile strength of post-tensioned cables is higher than hanger cables. The hanger cables were pre-anchored in the cable factory - Liuzhou OVM Company. The 37×15.5 mm post-tensioned cables were anchored in the bridge construction field. The EM sensors were manufactured in the Infrastructure Sensor Technology Laboratory of UIC and then shipped to cable factory and bridge construction field to mount on the cables. The pictures of the sensors and cables are shown in Fig. 6.

## 4. The calibration of EM sensors on hanger cables and post-tensioned cables

The EM stress sensors on hanger cables were calibrated using load cell in the laboratory, while those on post-tensioned cables were calibrated when the cables were loaded in bridge construction field, as load cells were mounted temporarily.

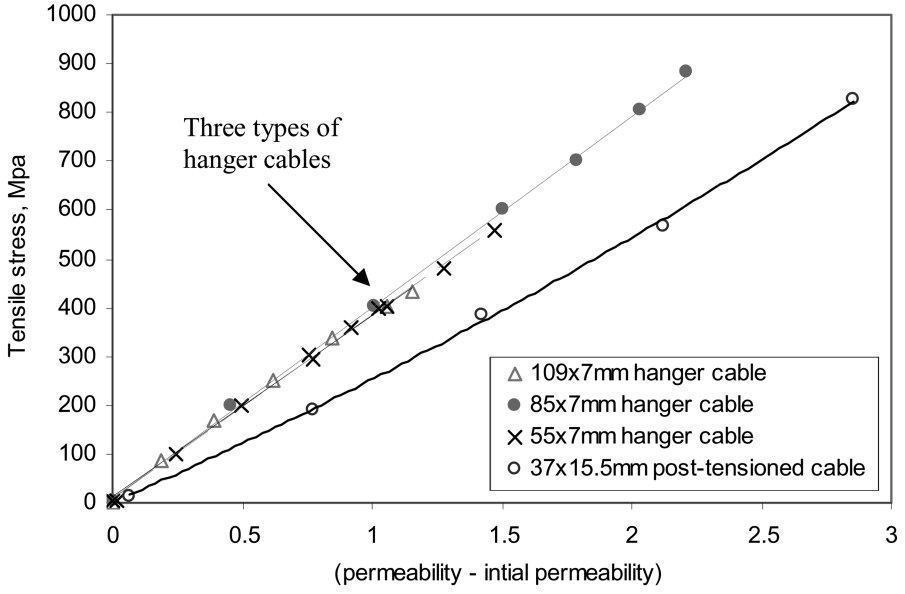


Fig. 7 Calibration curves of the EM sensors for different types of cables

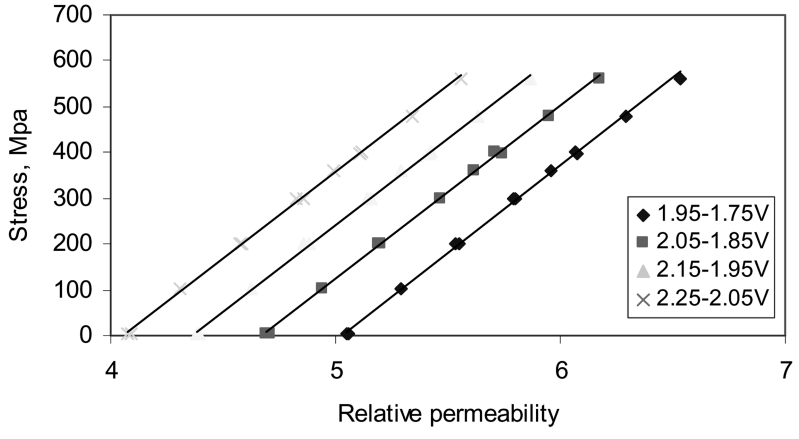


Fig. 8 Calibration curves of the EM sensor for 55×7 mm hanger cable with different working points

The hanger cables used in QJ 4th Bridge are similar in configuration but contain different number of parallel wires. Their calibration results are close to each other, as shown in Fig. 7. The calibration curves are parallel regardless of the variation in zero-stress reading (the permeability measured under zero external tension), as seen in Fig. 8. The repeatability and accuracy were guaranteed. For small EM sensors (currently are being mounted on a bridge in Maine, USA), the accuracy is about 1%, for EM sensors with inner diameter larger than 70mm, the accuracy is about 5%.

Two-dimensional calibration functions, including temperature compensation (see section 5 in this paper for temperature influence) were employed in *in situ* load monitoring. As the stress is dependent on the variation in relative permeability, the high repeatability of zero-stress reading is extremely

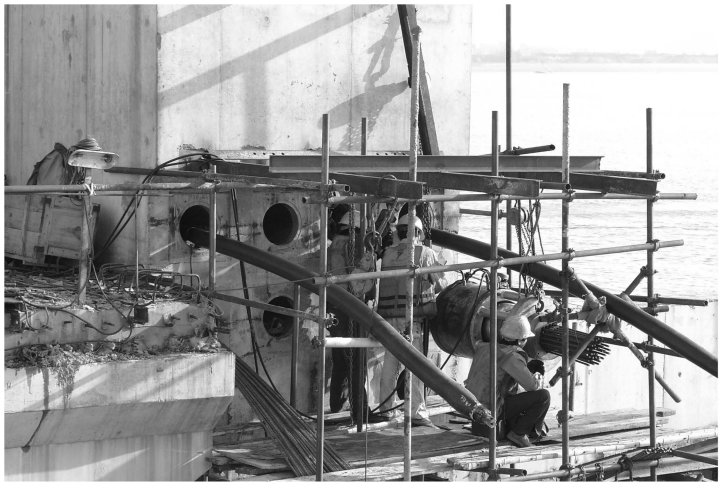

Fig. 9 Loading jack at the end of the post-tensioned cable

important. Studies indicated that there is an induction-stress hysteresis (Schneider and Cannell, *et al.* 1992), which is caused by thermal relaxation and diffusion aftereffect (Bertotti 1998). To stabilize the zero-stress reading, it is necessary to magnetically saturate the cable section near the location of the EM sensor by conducting several measurements prior to the final reading, as the diffusion aftereffect and the thermal relaxation can be diminished.

In order to load the 37×15.5 mm post-tensioned cables on bridge, hydraulic loading jack was mounted on the end of the cable, as shown in Fig. 9. Load cell was also mounted for loading control. The load cell would be dismounted when the cable was loaded to required level. The cable was pulled to 45% of the yielding strength. Therefore, the total elongation was around 880 mm for each cable. The loading process was divided into four steps. In each step, Load cell reading was recorded when the hydraulic pressure was maintained for at least three minutes to ensure stress stabilization. EM sensors on post-tensioned cables were calibrated with load cells.

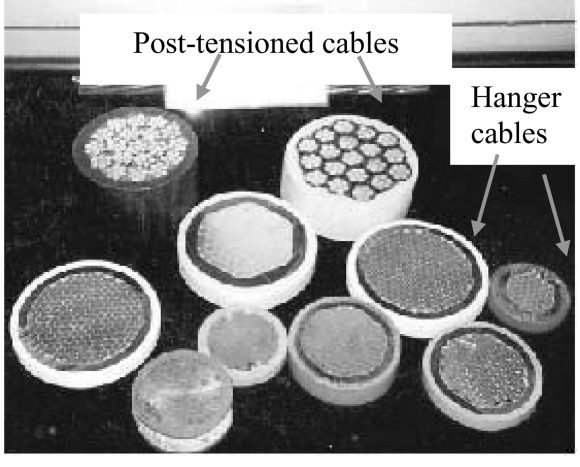


Fig. 10 Cross sections of various cables

Calibration results in Fig. 7 show that the monitoring function for hanger cables is the same, but different from that for the post-tensioned cables, due to the difference between hangers and post-tensioned cables in respect of the materials and configurations, as indicated in Fig. 10 In hanger cables, the galvanized wires contact each other, while in post-tensioned cables, each strand is covered with an anti-corrosive epoxy resin layer. Therefore, under energizing current pulse, the eddy current leads to larger magnetic field decay in hanger cables than in post-tensioned cables. For hanger cables composed of different number of wires, the consistency in calibration curves indicates that the existence of eddy current mainly depends on the type of material and the cable configuration. However, for cables with too small diameters or extremely large diameters, the eddy current patterns are so different that the magnetoelasticity must be calibrated respectively.

## 5. Temperature influence

Temperature has a tremendous influence on magnetization - First, according to Preisach theory (Bertotti 1992), the meta-stable energy and the energy profile of any individual Preisach unit are determined by the exchange, anisotropic, magnetic potential, and magnetostatic energy, which all demonstrate dependence on temperature. Second, thermal equilibrium is a kinetic process, and the time that the unit of material jumps from one minimum energy state to the other depends exponentially on the ratio of the energy barrier and $K_BT$, with $K_B$ indicating the Boltzmann constant, and $T$ being absolute temperature. Moreover, temperature determines the barrier energy against the domain wall movement and the wall-dislocation interaction range. Thermal expansion can also introduce micro strains to the materials (Birss 1971). As a result, temperature dramatically affects the magnetization curve, as indicated in Fig. 11.

Previous research indicates that temperature shifts the calibration curve in a parallel way (Chen 2000).

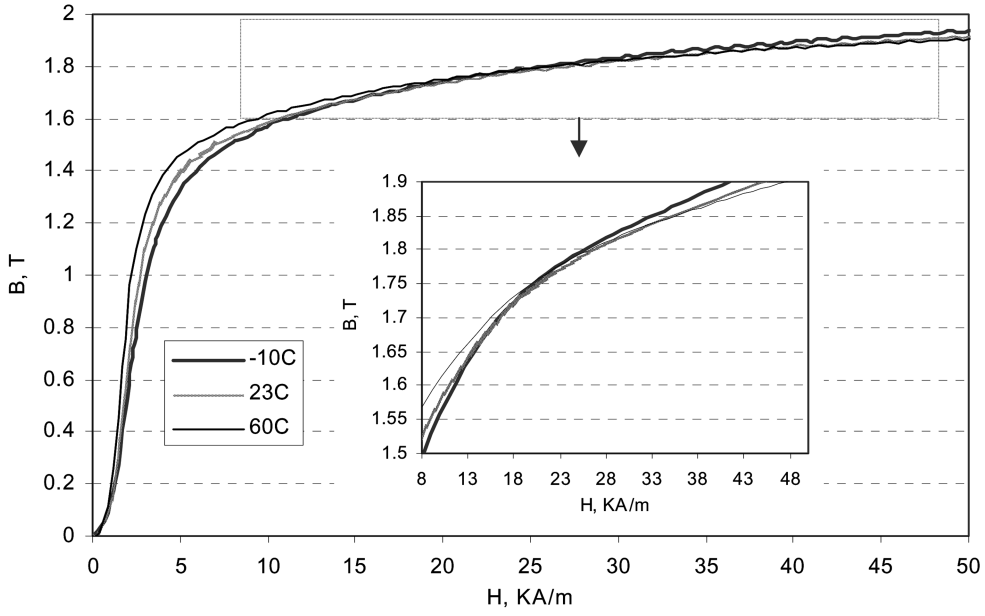


Fig. 11 Initiative magnetization curves of the 7 mm piano steel wire tested at different temperatures

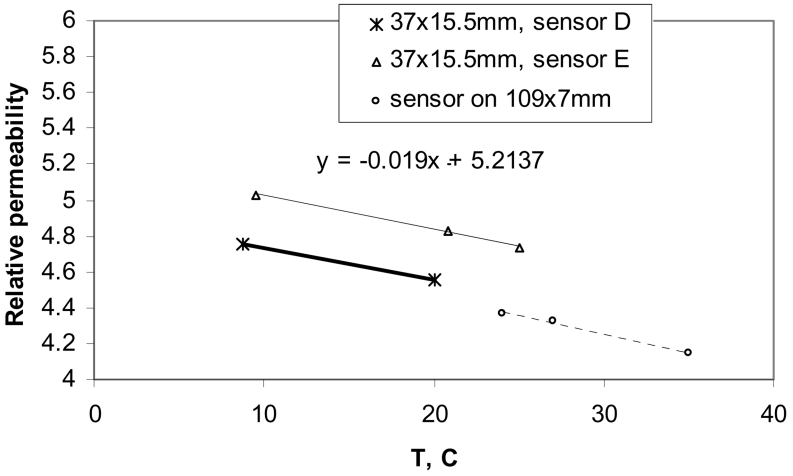


Fig. 12 $\mu(0, T)$ vs. T for hanger cable and post-tensioned cables

Therefore, to exclude the thermal influence, the effect of temperature on initial permeability (permeability under zero stress - $\mu(0, T)$ needs to be calibrated. Tests show that temperature dependence of the permeability is the same for hanger cables and multi-strand cables, as observed in Fig. 12, as the similarity of the materials leads to the same temperature dependence of magnetoelasticity. The dependence of permeability on stress $\sigma$ and temperature $T$ can be expressed as

$$\mu(H, \sigma, T) = \mu(H, 0, T_0) + m_1\sigma + m_2\sigma^2 + \alpha(T - T_0) \tag{9}$$

where $m_1$, $m_2$ and $\alpha$ are all calibration constants.

## 6. Tension monitoring results

EM sensors were calibrated using conventional measurements, as discussed in Section 4. The measurement of zero-stress reading is a prerequisite for tension monitoring, as indicated in Eq. (9). The sensors were mounted on the cables before they were anchored, so there is no problem to derive the zero-stress reading. However, for cables on existing bridges, we have different design of magnetoelastic sensor to monitor the tension, while this issue is not discussed in this paper. Tension in the cables was measured during construction and after the completion of construction. The atmospheric temperature was taken as the temperature of the cables. It is noted that there is a temperature gradient between atmosphere and steel. Lloyd, Singh and Wang (2002) studied the influence of the cable sheath on thermal flux and temperature homogenization, and they pointed out that the high-density polyethylene (HDPE) cover can cause a temperature difference of 4~5°C between the steel and ambient air, which incurs an error of around 25 Mpa. Therefore, the accuracy can be improved if the temperature of the steel is directly measured.

The EM sensor on the post-tensioned cable was calibrated during the loading process using load cell. When the bridge construction was completed, truck loading test was conducted and tension fluctuation in the post-tensioned cable was observed, as shown in Fig. 13.

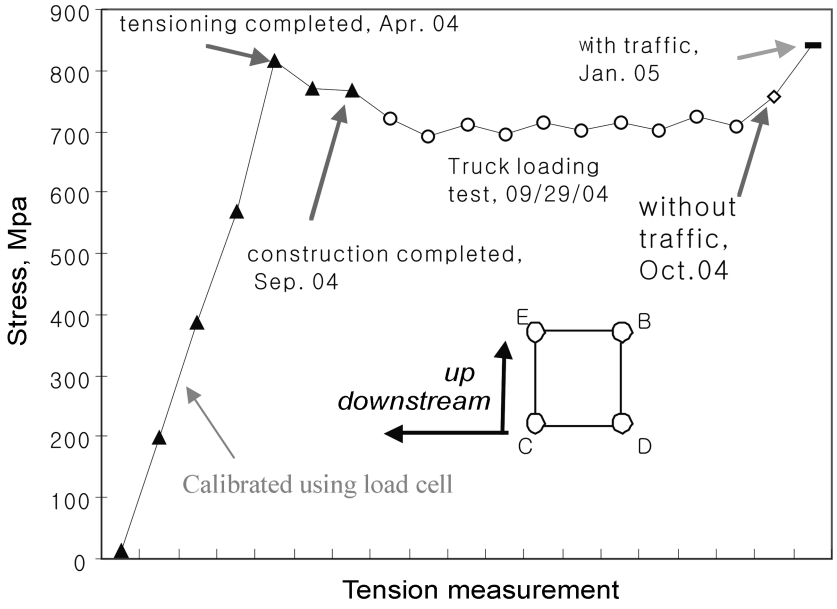


Fig. 13 Tension monitoring of post-tensioned cable (D), which is in the box girder of the north big arch

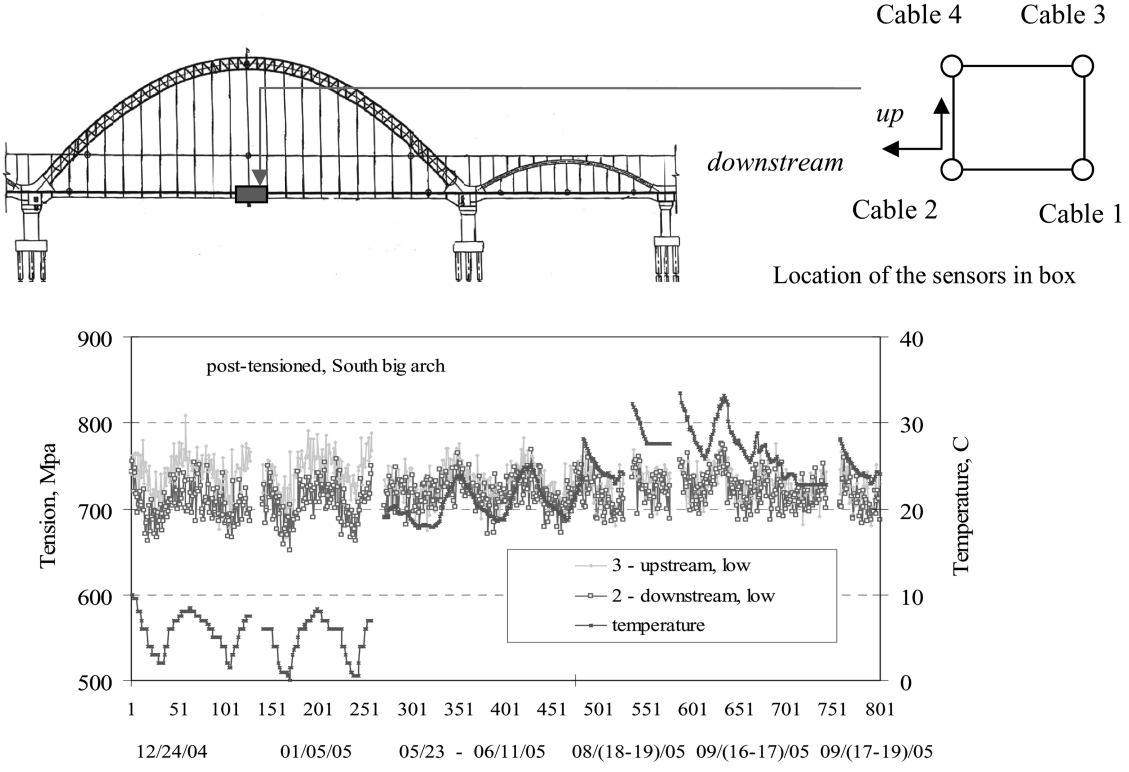


Fig. 14 Tension monitoring of post-tensioned cables on north big arch of QJ bridge

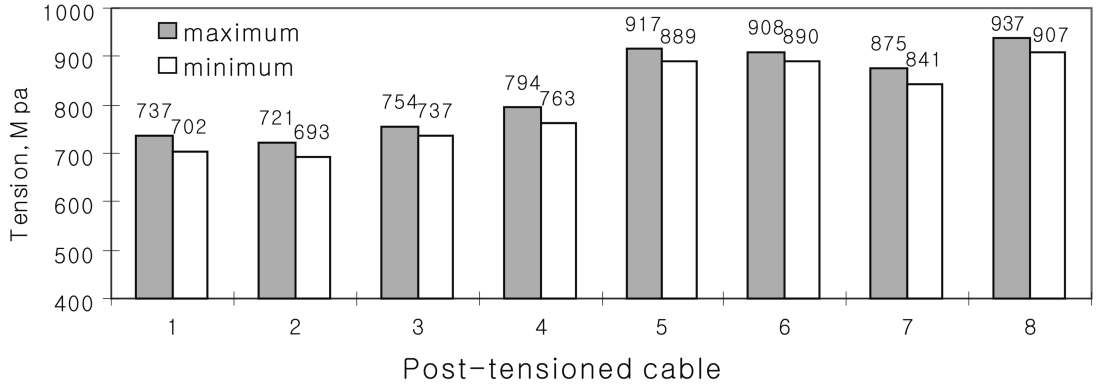


Fig. 15 Maximum and minimum tension of the post-tensioned cable with a day (JAN05 ~ JAN06), cable 1, 2, 3, 4 are in the box girder of north big arch, cable B, C, D, and E are on south big arch

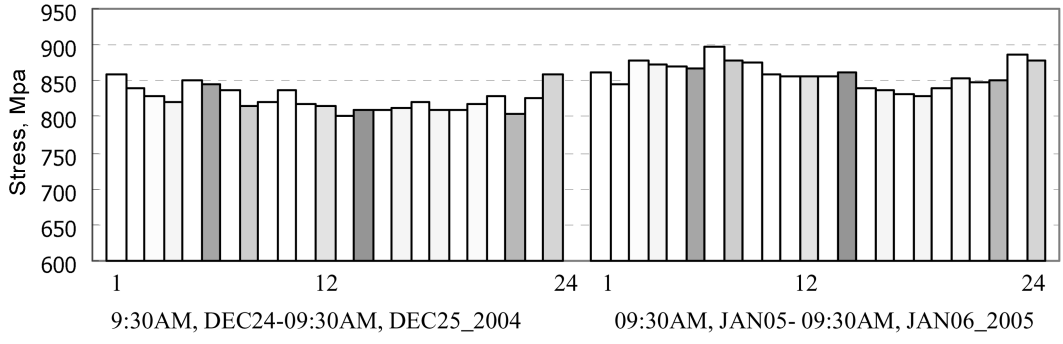


Fig. 16 Tension measurement of a post-tensioned cable (NO.D)

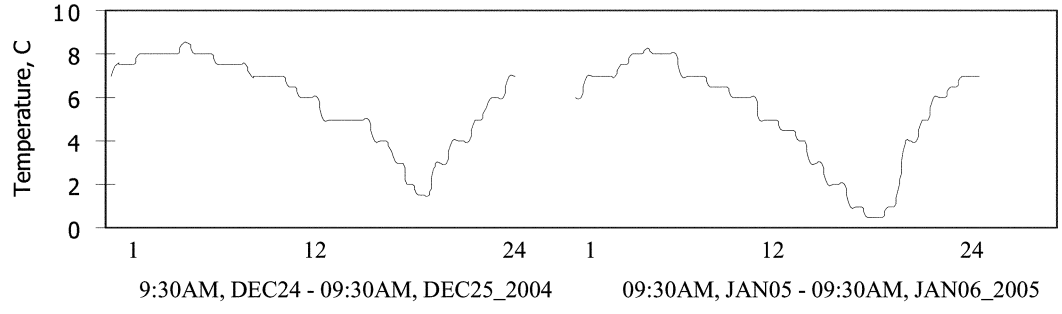


Fig. 17 Temperature measurements within two discontinuous days

The continuous tension variation in the post-tensioned cables was measured when the bridge was in service, as shown in Fig. 14 and Fig. 15. For the post-tensioned cables, tension increases with the drop of temperature. However, as observed in Fig. 16 and Fig. 17, the tension fluctuation did not coincide with ambient temperature, due to the temperature lag in the box girder housing the post-tensioned cables. For the hanger cables, tension varies with traffic, as shown in Fig. 18. It can also be observed that the cable in the center of the arch is subjected to the higher load. Fig. 19 and Fig. 20 demonstrate

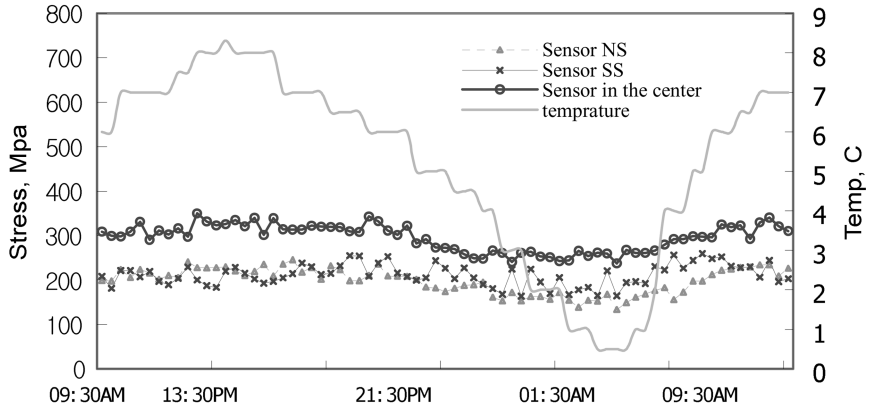


Fig. 18 Tension measurement (JAN05 ~ JAN06, 2005) of lower hanger cables on one big arch of the bridge, NS - north sensor near south pier, SS - south sensor near south pier

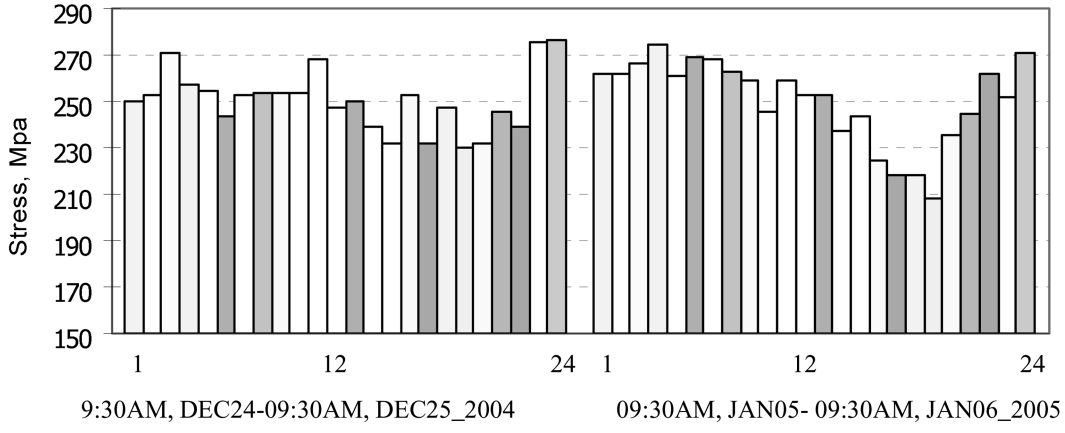


Fig. 19 Tension measurement of a 55×7 mm hanger cable on upper deck

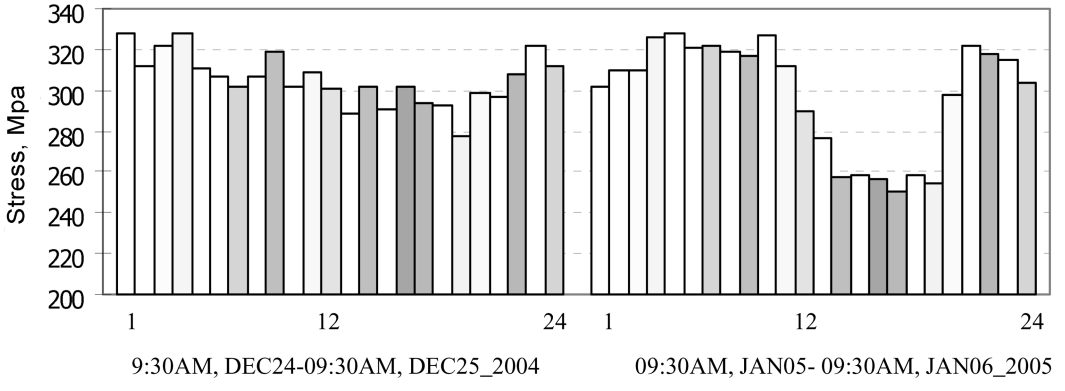


Fig. 20 Tension measurement of an 85×7 mm hanger cable (located at the center of south big arch) on lower deck

the tension variation of the hanger cables on upper and lower decks within two days. The traffic condition on bridge must be considered in tension analysis. It is noted that the EM stress sensors are used to monitor static stress or low-frequency stress fluctuation, as under stress fluctuation with high frequency, thermodynamic equilibrium can hardly be achieved, due to domain wall movement and carbon diffusion (Shewman 1989).

## 7. Conclusions

The magnetoelastic stress sensors for hanger cables and post-tensioned cables on QJ 4th Bridge were calibrated and tested. It has been shown that the stress dependence of the relative permeability is the same for hanger cables composed of parallel 7 mm piano steel wires. For post-tensioned cables, the stress dependence of permeability is different from that of hanger cables. This observation can be interpreted with eddy current distribution. From the view of engineering application, a small shift in zero-stress reading (also called initial permeability or permeability under zero stress) does not change the correlation of tension with permeability variation - permeability under stress minus zero-stress reading. Role of temperature was also calibrated. The tension monitoring results for the cables on the bridge was demonstrated. In order to monitor successfully the tensions in steel cables, attentions are to be given to the following aspects - (1) The stabilization of the magnetization is extremely important. (2) The same calibration curve can only be applied to the cables with same material and configuration, regardless of the diameters of the cables. However, cables with extremely large or small diameters must be calibrated separately. (3) The sensors suits for the monitoring of static stress or low-frequency stress fluctuation.

## Acknowledgements

The authors wish to thank Smart Structures, LLC for their financial support and Liuzhou OVM Company for their help in sensor calibration.

## References

Bozorth, R. M. (1951), Ferromagnetism, D. Van Nostrand Company, Inc., Canada.
Bertotti, G. (1992), *Hysteresis in Magnetism*, Academic Press Series in Electromagnetism, MD.
Birss, R. R. (1971), "Magnetomechanical effects in the Rayleigh region", *IEEE Trans. Magn.*, **7**, 113-133.
Chen, Z. (2000), "Characterization and constitutive modeling of ferromagnetic materials for measurement of stress", PhD thesis, the University of Illinois at Chicago.
Cullity, B. D. (1972), *Introduction to Magnetic Materials*, Addison-Wesley Publishing Company, Reading MA.
Daughton, J. M. (1999), "GMR applications", *J. Magn. Magn. Mat.*, **192**, 334-342.
Griffiths, D. J. (1999), *Introduction to Electrodynamics*, 3rd Edition, Prentice Hall, Inc.
Hovorka, O. (2002), "Measurement of hysteresis curves for computational simulation of magnetoelastic stress sensors", MS thesis, the University of Illinois at Chicago.
Jiles, D. C., Lo, C. C. H. (2003), "The role of new materials in the development of magnetic sensors and actuators", *Sensors and Actuators A*, **106**, 3-7.
Lloyd, G. M., Singh, V., Wang, M. L. (2002), "Experimental evaluation of differential thermal errors in magnetostatic stress sensors for Re < 180", *IEEE Sensors 2002*, Magnetic Sensing III, Paper No. 6.54.

Mix, P. E. (1987), *Introduction to Non-destructive Testing*, John Wiley & Sons, Inc., Hoboken, NJ.
Joule, J. P. (1842), "On a new class of magnetic forces", *Ann. Electr. Magn. Chem.*, **8**, 219-224.
Schneider, C. S., Cannell, P. Y. and Watts, K. T. (1992), "Magnetization for large stresses", *IEEE Trans. Magn*, **28**, 2626-2631.
Shewman, P. (1989), *Diffusion in Solid*, 2nd edition, Mineral, Metals & Materials Society, Warrendale, PA.
Singh, V., Lloyd, G. D., Wang, M., L. (2003), "Effects of temperature and corrosion thickness and composition on magnetic measurement of structural steel wires", *the 6th ASME-JSME of 2003*.
Stablik, M. J. and Jiles, D. C. (1993), "Coupled magnetoelastic theory of magnetic and magnetostrictive hysteresis", *IEEE Trans. Magn.*, **29**, 2113-2123.
Tayalia, P., Heider, D. and Gillespie, J. W. Jr. (2000), "Characterization and theoretical modeling of magnetostrictive strain sensors", *Sensors and Actuators A*, **111**, 267-274.
Wang, G. and Wang, M. L. (2004), "The utilities of U-shape EM sensors in stress monitoring", *Struct. Eng. Mech.*, **17**(3-4), 291-302.
Wang, M. L., Chen, Z. L., Koontz, S. S. and Lloyd, G. D. (2000), "Magneto-elastic permeability measurement for stress monitoring", *Proceeding of the SPIE 7th Annual Symposium on Smart Structures and Materials, Health Monitoring of the Highway Transportation Infrastructure*, 6-9 March, CA, **3995**, 492-500.
Wang, M. L., Koontz, S. and Jarosevic, A. (1998), "Monitoring of cable forces using magneto-elastic sensors", *2nd U.S. -China Symposium Workshop on Recent Developments and Future Trends of Computational Mechanics in Structural Engineering*, May 25-28, Dalian, PRC, 337-349.
Wang, M. L., Lloyd, G. and Hovorka, O. (2001), "Development of a remote coil magneto-elastic stress sensor for steel cables", *SPIE 8th Annual International Symposium on Smart Structures and Material, Health Monitoring and Management of Civil Infrastructure Systems*; Newport Beach CA, **4337**, 122-128.
Weiss, P. (1907), "Hysteresis of the molecular field and ferromagnetic properties", *J. Phys.*, **4**, 661-690.

*VG*